J. Electrochem. Sci. Eng. **9(2)** (2019) 99-111; http://dx.doi.org/10.5599/jese.639

Open Access: ISSN 1847-9286
www.jESE-online.org

Original scientific paper

Effect of immersion time on electrochemical behavior of the stainless steel AISI 304 - 0.01 M chloride solution interface

Wejdene Mastouri, Luc Pichon, Serguei Martemianov, Thierry Paillat, Anthony Thomas✉

Institut Pprime, Université de Poitiers-CNRS-ENSMA, UPR 3346, Poitiers, France

✉Corresponding author: anthony.thomas@univ-poitiers.fr

Received: November 20, 2018; Accepted: February 2, 2019

Abstract

Stainless steels are broadly used thanks to their specific physical properties such as their high corrosion resistance in poorly aggressive solutions. However, only few studies have been reported in the literature concerning their electrochemical behavior in low concentration electrolytes medium. Accordingly, the present work aims to study the immersion time influence on the solid-liquid interface properties of the austenitic stainless steel AISI 304L, immersed in a low-concentrated (0.01 M) sodium chloride (NaCl) solution. The electrochemical behavior of the interface was evaluated by electrochemical impedance spectroscopy (EIS) and open circuit potential (OCP) monitoring. The morphological features and the modification of the surface composition were evaluated by optic microscopy, scanning electron microscopy, energy dispersive X-ray spectrometry, atomic force microscopy, white light interferometry and X-ray photoelectron spectroscopy. It was determined by OCP measurement that the characteristic time of the interface stabilization is very long (several months). After an immersion of 2 months in NaCl solution, a second time constant on impedance phase diagram appears. Surface characterizations reveal a significant modification of the morphology and chemistry of the AISI 304L surface that can be linked to OCP/EIS observations. It can be noticed that the repeatability deviation of the EIS method was about 1 % while its reproducibility deviation was estimated to 35 %.

Keywords

Stainless steel AISI 304L; Low concentration sodium chloride solution (0.01 M); Electrochemical Impedance Spectroscopy; X-ray Photoelectron Spectroscopy; Immersion time effect

Introduction

Austenitic stainless steels (ASS) are widely used nowadays for a great number of applications thanks to their ability to resist in corrosive environments while keeping good mechanical properties.

The corrosion resistance of ASS originates from the protective chromium-rich passive film formed spontaneously on the surface when it is exposed to air. The passive film consists of an external part enriched in iron/chromium hydroxides and an internal part enriched in oxides [1,2]. Its thickness is limited to few nanometers and its composition depends on the conditions of preparation and on the surrounding medium [3]. However, the passive film is heterogeneous and presents a highly disordered or even amorphous structure [4]. The presence of this passive oxide layer, usually with a semiconductor electric behavior, has to be obviously taken into account in the study of the solid/liquid interface.

When an alloy surface is immersed in liquid, serious difficulties such as non-stability, roughness or non-uniformity of the surface may be encountered during its study. These issues consequently induce a low repeatability and reproducibility of the measurements.

In this work, the studied interface is composed of a polycrystalline austenitic stainless steel AISI 304L (ASS 304L) immersed in a low concentrated sodium chloride solution (0.01 M). The goal of this paper is to investigate the immersion time influence on the interface properties by combining electrochemical and surface characterization techniques. Last decades, stainless steel/electrolytic solution interface has been extensively studied in corrosive conditions, with high concentrations of the electrolyte [5,6]. Nonetheless, to our knowledge, only few studies concern the electrochemical behavior of stainless steels in contact with low concentration electrolytes and in an electrical potential range where the contribution of faradic reactions may be considered weak [7,8]. The morphology and the chemical composition of ASS 304L samples surfaces were examined by optic microscopy (OM), scanning electron microscopy (SEM), energy dispersive X-ray spectrometry (EDS), atomic force microscopy (AFM), white light interferometry (WLI) and X-ray photoelectron spectroscopy (XPS).

Experimental

Material and solution

ASS 304L is an iron-based alloy with two main alloying elements: chromium and nickel. The studied ASS 304L is mainly crystallized in the austenitic face centered cubic (FCC) *γ* phase, with grain sizes of few tens of micrometers. Some different precipitates (carbides, MnS, …) exist, as well as some residual ferritic *α* phase grains. The samples for electrochemical measurements consist of 5.0 × 4.0 mm (diameter × thickness) cylinders. The chemical composition of this steel provided by the supplier Goodfellow® and confirmed by EDS (except the carbon content) is shown in Table 1.

Table 1. *Chemical composition of the ASS 304L used in this study*

Content, wt.%					
Fe	Cr	Ni	Mn	C	Mo
Bal.	18.14	8.08	1.77	0.024	0.3

To obtain reproducible electrochemical results, the ASS 304L electrode was carefully prepared by a dedicated polishing process. Samples were initially mechanically polished with increasing grade (500 to 2000) silicon carbide (SiC) papers, then with 6 to 1/4 µm diamond suspension abrasives. To eliminate the polishing residues, specimens were degreased in a commercial RBS™ 25 detergent solution, washed with tap water, distilled water and then rinsed with ethanol in ultrasonic bath. They were finally dried under a low nitrogen flow at ambient temperature.

All the electrochemical experiments were carried out in 0.01 M NaCl solutions with pH equal to 6 ± 0.5 at T = 20 °C. The reason of using these molar concentrations is to avoid corrosion problems.

The solutions were prepared with ultra-pure water, produced and purified with Millipore-Milli-Q system, and were used immediately after their preparation to avert contamination.

Electrochemical experiments

All electrochemical experiments were carried out in a conventional three-electrode cell. The cell is a cylindrical Pyrex® glass of 100 mL capacity, double walled, allowing water circulation to keep the temperature of the cell constant at 17.0 ± 0.2 °C thanks to a thermostatic bath. Before each measurement, the cell was cleaned with pure water and rinsed with the electrolytic NaCl solution. A saturated Ag/AgCl and a platinum slab of 2 cm^2 were used as the reference electrode and counter electrode, respectively. All potential measurements presented in the present study are thus referred to the Ag/AgCl potential. The working electrode was a polished ASS 304L cylinder. It was fixed in a PTFE holder, keeping only the top surface of the cylinder (0.2 cm^2 area) exposed to the electrolyte. The working electrode was embedded on a rotating disk electrode (RDE) providing a controlled liquid flow to avoid diffusion-limited phenomena. Before starting each electrochemical experiment, the electrolyte was previously deaerated by nitrogen bubbling for 20 min in order to reduce the dissolved oxygen content. The nitrogen circulation at the edge of the free surface of the solution was maintained during all measurement duration. A Solartron® Multistat 1480 potentiostat/galvanostat, coupled with a model 1260 frequency response analyzer was employed to perform the electrochemical measurements.

The monitoring of OCP evolution over few hours was performed after various immersion times: less than 25 minutes, 3 days and 2 months.

Electrochemical Impedance Spectroscopy (EIS) experiments were carried out by applying, at open circuit potential (0 V) vs. Ag / AgCl, a perturbative sinusoidal potential with amplitude of 10 mV. The impedance response was measured over frequencies from 10^4 Hz to 0.5 Hz.

Surface characterization

A Nikon® optical microscope and a JEOL-TTLS 7001F field emission gun scanning electron microscope (FEG-SEM) equipped with an energy dispersive spectroscopy (EDS) microanalysis hardware (Oxford Instruments) were used in order to examine the morphology and the chemical composition of the surface before and after immersion in chloride containing solutions.

The roughness was evaluated by atomic force microscopy (AFM) on a Nanoscope III apparatus (Digital Instruments), operating in tapping mode on a 40×40 µm² surfaces, and by white-light interferometry (WLI) on a Talysurf CCL microscope (Taylor Hubson Ltd) on 350×350 µm² surfaces. The surface roughness of each specimen has been evaluated as the root mean square (RMS) value Rq.

Surface analyzes by XPS were realized with a Riber Division Instruments spectrometer using a non-monochromated Mg Kα X-ray line ($h\nu$ = 1250 eV) obtained with an accelerating voltage of 12 kV and a current intensity of 15 mA. The XPS analysis was performed under pressure of about 10^{-11} Torr. The incidence angle is 20° relative to the sample surface whereas the emitted photoelectrons are collected at θ = 20° from the surface normal direction. Although they may not be the most adapted to this study, these angles are fixed by the set-up geometry and cannot be modified. The deconvolution of the peaks was performed with Unifit 2007® software. The Shirley method was used for background subtraction. The energy positions were corrected in reference to the 1s carbon peak (284.6 eV binding energy) in order to eliminate any perturbation (charge effects, surface state, etc.). For each experimental peak, the fitting was realized with a small number of contributions (typically 3 or 4), using a Gaussian–Lorentzian product function, with relatively large FWHMs (full width at the half maximum) up to few eV, and deviation from a central binding energy up to 0.8 eV.

By considering that the Cr and Fe metallic contributions (Fe^0 and Cr^0) in the Fe2p and Cr2p peaks are exclusively coming from the bulk material under the oxide, the thickness of the passive film, δ_{ox} / Å, can be evaluated from the Eq. (1) [9].

$$\delta_{ox} = \lambda \cos\theta \ln\left\{\left(\frac{S_{Fe}N_{Fe}^{ox}I_{Cr}^{ox} + S_{Cr}N_{Cr}^{ox}I_{Fe}^{ox}}{S_{Fe}N_{Fe}^{m}I_{Cr}^{m} + S_{Cr}N_{Cr}^{m}I_{Fe}^{m}}\right)\left(\frac{N_{Cr}^{m}N_{Fe}^{m}}{N_{Cr}^{ox}N_{Fe}^{ox}}\right)+1\right\} \quad (1)$$

λ / Å is the average inelastic mean free path of photoelectron in the passive film (12.3 Å). θ is the collection angle (20° from the normal surface). S_{Fe}(0.188) and S_{Cr} (0.155) are the sensitivity factors of Fe and Cr elements, respectively. I_{Fe}^{Ox} and I_{Cr}^{Ox}, are respective area values of the oxide+hydroxide contributions in the Fe and Cr peaks. I_{Fe}^{m} and I_{Cr}^{m} are the area values of the metallic contribution (Fe^0 and Cr^0), respectively. N_{Fe}^{Ox} and N_{Fe}^{Ox} / mol m^{-3} are molar concentrations of *Fe* and Cr metal elements in passive film considered as a Fe_2O_3-Cr_2O_3 mixture (the Fe/Cr ratio in the oxidized film is given by the XPS quantification). N_{Fe}^{m} and N_{Cr}^{m} / mol.m^{-3} are molar concentrations of Fe and Cr metal elements in the unoxidized (bulk) alloy (ASS 304L).

No other special preparation of the surface (*e.g.* surface cleaning by ion beam sputtering) than the aforementioned post-polishing cleaning was carried out to obtain an analysis reflecting more closely the state of our surface before/after immersion. All physical and electrochemical measurements were performed before 48 hours interval after surface preparation.

Results and discussion

Surface analysis

Figures 1a and 1b show the surface of the ASS 304L observed with optic microscopy (OM) and scanning electron microscopy (SEM) before immersion in the NaCl solution and the electrochemical tests. The surface preparation allows to distinguish the presence of precipitates and γ grains with different crystallographic orientations (Figure 1a). Depending on the samples, some traces of residual scratches may still be visible at different scales of observation.

A large density of inclusions (highlighted by the red circle) could also be observed on the ASS 304L surface (Figure 1b). These inclusions have an average size ranging between 0.5 and 2 µm and are randomly distributed over the entire surface. The chemical analysis obtained by EDS (Figure 1c) revealed that the composition of these inclusions is richer in Mn and S (or unlikely Mo) compared to the spectrum obtained on a *γ* phase grain. A study on a 304L stainless steel immersed in alkaline solutions of NaOH + KOH in the presence of chlorides proposed by Freire et al. [6] highlights the presence of similar inclusions on the surface. According to this study as well as others [10], these inclusions have been identified as sulfides mixtures of MnS, CrS and/or FeS.

The RMS roughness value measured by WLI on several samples varies between 15 and 35 nm from one sample to another. The average roughness was evaluated to be 25 ± 10 nm. The average roughness value obtained by AFM is lower (13 ± 7 nm) mainly because the studied surface is smaller: 0.12 mm² in WLI versus 1.6.10^{-3} mm² in AFM.

The chemical composition of the passive film formed in presence of ambient air was assessed by XPS. The global surveys are presented in Figure 2a. Only the elements iron, chromium, oxygen and carbon can be clearly identified. The preponderance of the elements (C, O) is naturally relative to the oxide film and to the organic pollution of the surface. This is unavoidable with the preparation method used before XPS analysis (samples are kept in air for several hours and no sputtering was performed to clean the surface).

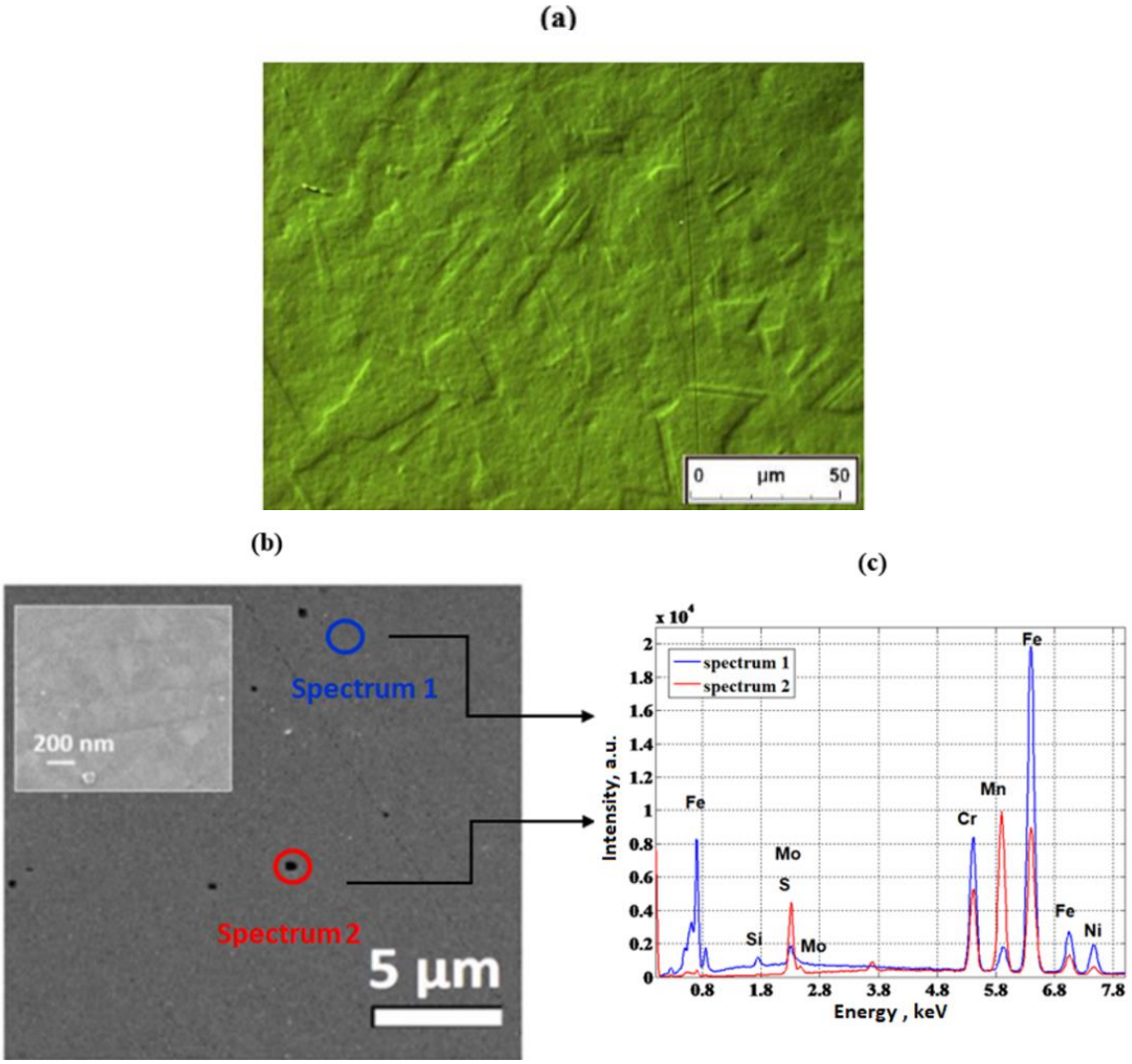

Figure 1. *(a) Optical microscope image (Nomarsky constrast), (b) scanning electron microscopy (secondary electron) image of ASS 304L surface, (c) EDS spectra registered on the austenitic grains (spectrum 1) and on the precipitate (spectrum 2)*

The other components of the alloy (Ni, Mn…) are not sufficiently visible outside the background noise because of a too low signal/background ratio. Indeed, nickel should appear at a binding energy of about 800 eV. However, in our case study, the Ni signal is quite low. Its weak signal can be explained by a relatively low concentration in the bulk material (few at.%), a significant organic pollution at the surface which shielded the signal but also by its low participation in the oxide layer probed by the XPS. Moreover, according to Veleva *et al.* [11], it is probably hidden by the Auger features of the other dominant metal oxides.

Figure 2 (b-e) shows the high resolution spectra of the normalized peaks Fe $2p_{3/2}$, Cr $2p_{3/2}$, O 1s and C 1s. XPS peak position and quantitative contents of the elements are listed in Table 2. Based on the deconvolution of the spectra, the passive film formed on the ASS 304L surface in contact with air is composed of oxides (FeO, Fe_2O_3, and Cr_2O_3) and hydroxides (FeOOH and $Cr(OH)_3$) of the two main metallic elements, Fe and Cr [12,13].

In the quantitative analysis (excluding carbon contaminants), a preponderance of chromium (3.14 at.%) on iron (1.82 at.%) was found in the layer probed by the XPS. The ratio Fe/Cr (all contributions combined) is about 0.58, whereas the expected value is 3.9 for the bulk material. This reflects the important role of chromium in the development of the native and passive oxide films.

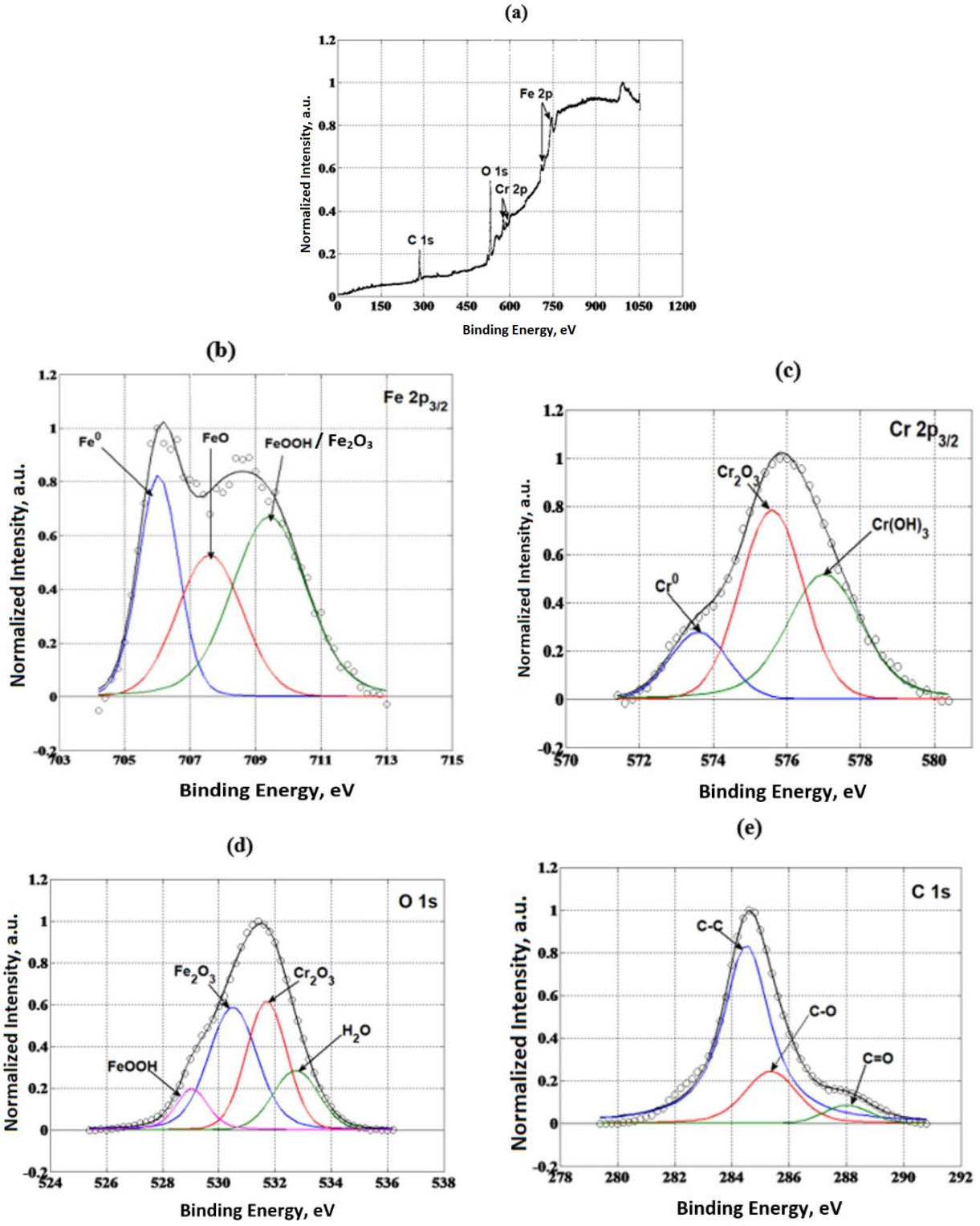

Figure 2. *(a) Low resolution survey XPS normalized spectrum and high resolution, (b) Fe $2p_{3/2}$, (c) Cr $2p_{3/2}$, (d) O 1s, (e) C 1s XPS normalized spectra of the ASS 304L surface after mechanical polishing. Experimental data are represented as round dots and lines refer to the different contributions and to the global optimized simulation*

In the hypothesis that Fe^0 and Cr^0 contributions are coming from the bulk material, and that oxides and hydroxides contributions are coming from the passive layer, the oxidized film thickness, calculated from the Eq. (1), corresponds approximately to 3.8±0.8nm. The uncertainty given here comes from the different possible hypotheses on the nature of the oxides and hydroxides (especially on their density).

Table 2. *Parameters used for the deconvolution of XPS spectra: the elements compositions, Fe/Cr ratio and thickness value of the passive film formed on ASS 304L in the air and after different immersion times*

		ASS 304L, in contact with air			ASS 304L, after immersion in 0.01 M NaCl solution (t = 0)			ASS 304L, after immersion in 0.01 M NaCl solution (t =2 months)		
Element	Detected species	Binding energy, eV	Element content by species, at.%	Element content, at.%	Binding energy, eV	Element content by species, at.%	Element content, at.%	Binding energy, eV	Element content by species, at.%	Element content, at.%
Fe $2p_{3/2}$	Fe^0 (metal)	706.1	0.50	1.82	705.6	0.19	1.30	705.7	0.11	0.55
	FeO	707.6	0.51		707.6	0.51		707.6	0.23	
	$FeOOH/Fe_2O_3$	709.4	0.80		709.3	0.60		709.4	0.21	
$Cr2p_{3/2}$	Cr^0 (metal)	573.6	0.47	3.14	573.9	0.46	1.89	573.0	0.28	2.42
	Cr_2O_3	575.6	1.43		575.1	0.67		575.2	1.06	
	$Cr(OH)_3$	577.0	1.24		576.4	0.77		576.5	1.09	
O 1s	FeOOH	529.1	18.64	46.28	529.0	13.13	48.42	529.0	11.81	29.10
	Fe_2O_3	530.5	15.30		530.6	17.81		530.4	8.77	
	$Cr_2O_3/Cr(OH)_3$	531.7	7.95		531.5	10.19		531.6	5.47	
	H_2O	532.7	4.39		532.5	7.28		532.7	3.05	
C 1s	C -C	284.6	36.14	48.76	284.6	30.46	48.39	284.6	45.55	67.94
	C - O	285.4	9.85		285.2	10.06		285.2	18.77	
	C = O	288.1	2.77		288.0	1.87		287.4	4.61	
Fe / Cr			0.58			0.69			0.23	
δ_{ox} / nm			3.8 ± 0.8			3.5 ± 0.8			4.1 ± 0.8	

Electrochemical impedance spectroscopy (EIS)

The impedance experimental diagrams obtained on the ASS 304L alloy tested in the NaCl solution are shown in Figure 3. They highlight similar behavior as those reported in the literature for stainless steel electrodes immersed in a low concentration electrolytic solution [7,8].

In the quantitative analysis (excluding carbon contaminants), a preponderance of chromium (3.14 at.%) on iron (1.82 at.%) was found in the layer probed by the XPS. The ratio Fe/Cr (all contributions combined) is about 0.58, whereas the expected value is 3.9 for the bulk material. This reflects the important role of chromium in the development of the native and passive oxide films.

On the Nyquist diagrams in Figure 3 (a,d), a near-vertical line corresponding to a predominantly capacitive behavior is obtained. The line tilt reflects the presence of secondary faradic reactions arising from impurities in the electrode and the electrolyte. By increasing the frequency, the interface switches from a capacitive to a resistive behavior characterized by a phase ($-\theta$) approaching zero and a constant impedance module (Fig. 3 b,c,e,f). The phase angle evolution with frequency presented in Figure 3 (c,f) shows that the phases are lower than 90°, for all impedance spectra. Such behavior can be interpreted as a deviation from the ideally polarized blocking electrode behavior.

Repeatability and reproducibility tests

Reproducibility and repeatability constitute a major challenge during solid/liquid interfaces studies. To show the repeatability, at least three series of measurements were performed the same day, one after the other, on the same sample, with the same electrolytic solution. For the reproducibility, it consists to reproduce each electrochemical measurement several times on several different specimens changing each time the used solution. For this purpose, three samples were identically prepared, on different days and consequently under slightly different conditions (room temperature, products amount used for polishing, *etc*.).

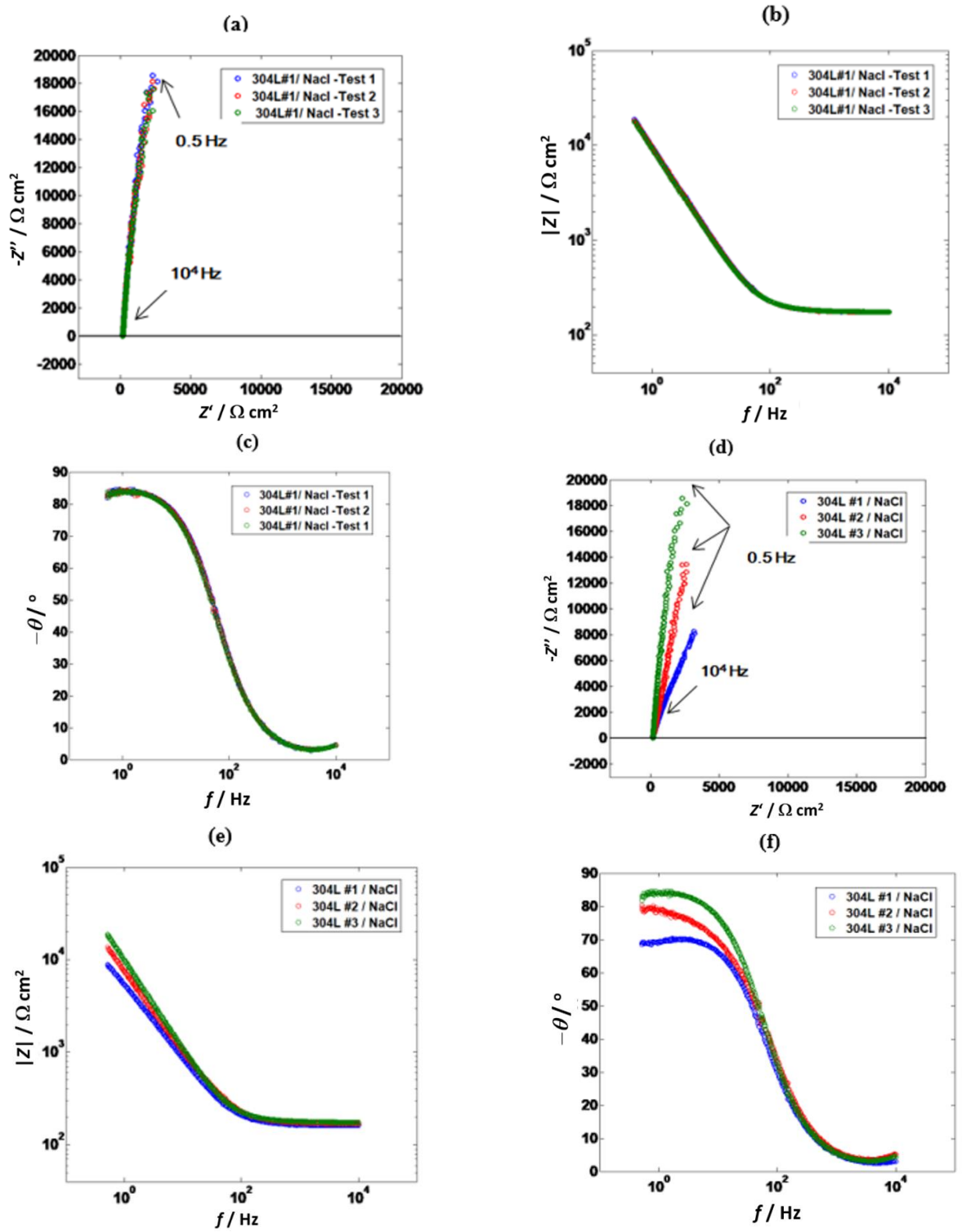

Figure 3. (a-c) *Repeatability,* ***(d-f)*** *Reproducibility of electrochemical impedance measurements obtained with ASS 304L in NaCl solution (0.01M) at E= 0 V* vs. *Ag/AgCl:* ***(a,d)*** *Nyquist and* ***(b,c,e,f)*** *Bode plots.*

According to Figure 3 (a,b,c) the repeatability deviation is about 1 %, demonstrating very good repeatability of the results with unique sample. Considering the reproducibility tests shown on Figure 3 (d,e,f), the obtained deviation remains high in the order of 35 %. The high dispersion can be related to the nature of the material used which is a polycrystalline alloy of different elements, presenting heterogeneities at the surface and different grains with variable crystallographic orientations. The actual state of the surface, especially its morphology, cannot therefore be strictly the same for different samples. Other factors could also generate a decrease in reproducibility such as the quality of the electrolyte.

Effect of immersion time

Immersion time is one of the most influential parameter on interface properties. Results on stainless steel related to short-term tests have been widely discussed in literature [5-6,14-15], however little has been carried out for relatively long contact periods between the electrolyte and the metallic material [16,17].

Open circuit potential evolution

Figure 4 illustrates the OCP evolution for the ASS 304L in the NaCl solution measured just after the immersion in liquid (t=0), after an immersion of 3 days (t = 3 days) or after an immersion time up to 2 months (t = 2 months). The alloy exhibits an increase of OCP with time. Nonetheless, a non-stabilized profile and strong fluctuations are remaining even after 3 days of immersion. Thus, the time required to reach the stationary state is relatively long (higher than several days). For the test realized after a 2 months' immersion, the OCP values evolve smoothly between -0.1 and 0.075 V *vs* Ag/AgCl during the first 6 hours (21600 s) and stabilize around 0.075 V over the other 25 hours of measurements (115000 s).

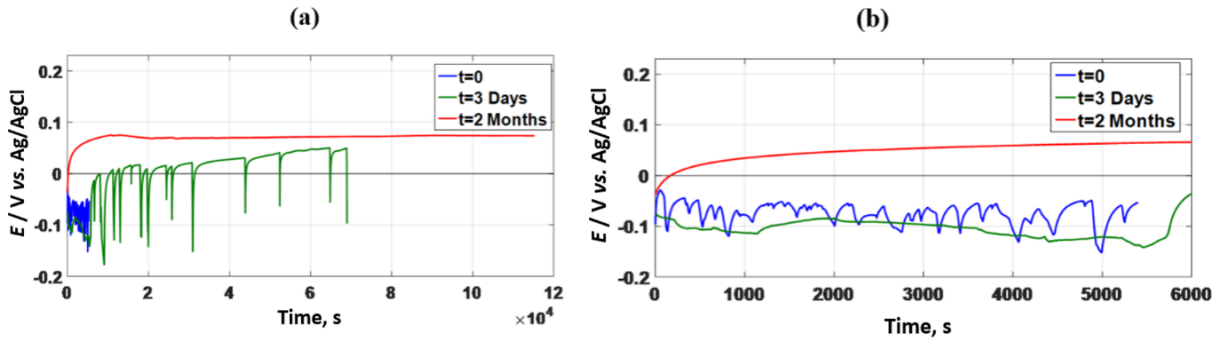

Figure 4. *(a) Open Circuit Potential evolution of the ASS 304L from 0 to 2 months of immersion in the NaCl solution (0.01M), (b) zoom on the first 6000 s of measurements*

The OCP stabilization at a value of 0.075 V *vs.* Ag/AgCl was verified only after a long period of 2 months. Although a follow-up of the OCP evolution at different times between 3 days and 2 months would be necessary to accurately define the OCP stabilization, this result suggests that the time constant of the interface stabilization is in the order of at least several days. According to Mohammedi *et al.* [5], OCP values stabilize at higher immersion times due to the nonlinear rate of oxide film growth.

Impedance spectroscopy analysis after long-term solution immersion

EIS data were recorded after two different immersion times, t = 0 and t = 2 months and presented in Figure 5. Bode plots show that the first time constant is shifted to higher frequencies and a second time constant τ_2 appears at low frequency (< 10 Hz) when the immersion time is increased from 0 to 2 months.

This behavior can be related to the passive film. Indeed, a film evolution according to the immersion time can be noted. Time constant τ_2 can also be attributed to the charge transfer related to the electrical double layer (EDL) developing at the passive film/NaCl interface.

Surface analysis of passive films on stainless steel ASS 304L after long-term solution immersion

The SEM images of the ASS 304L surface morphology after the first immersion (less than 25 minutes, t=0) does not present any new features compared to the initial surface (Figure 6a).

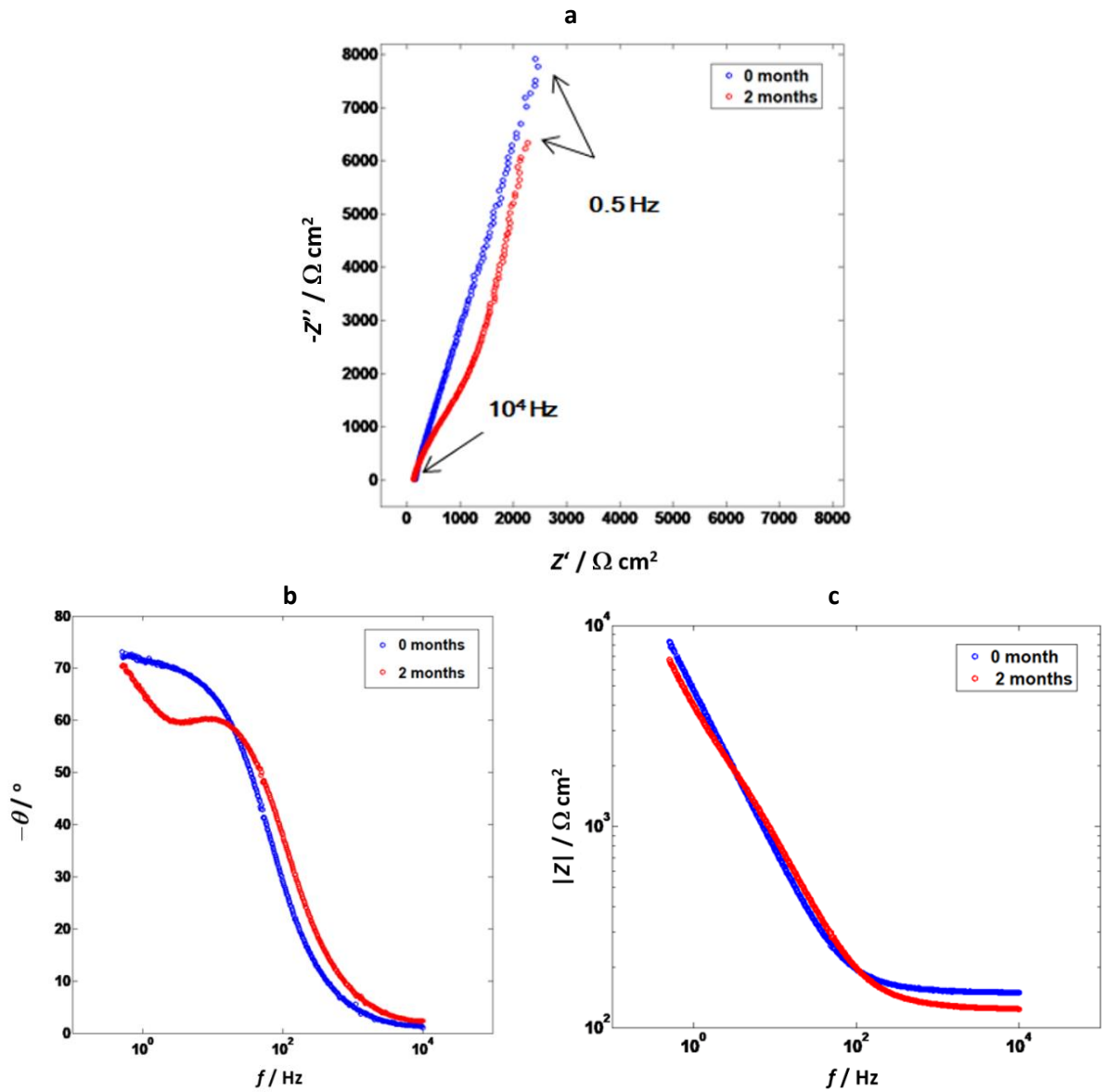

Figure 5 *(a) Nyquist and (b-c) Bode plots obtained for ASS 30NaCl solution (0.01M) after different immersion times*

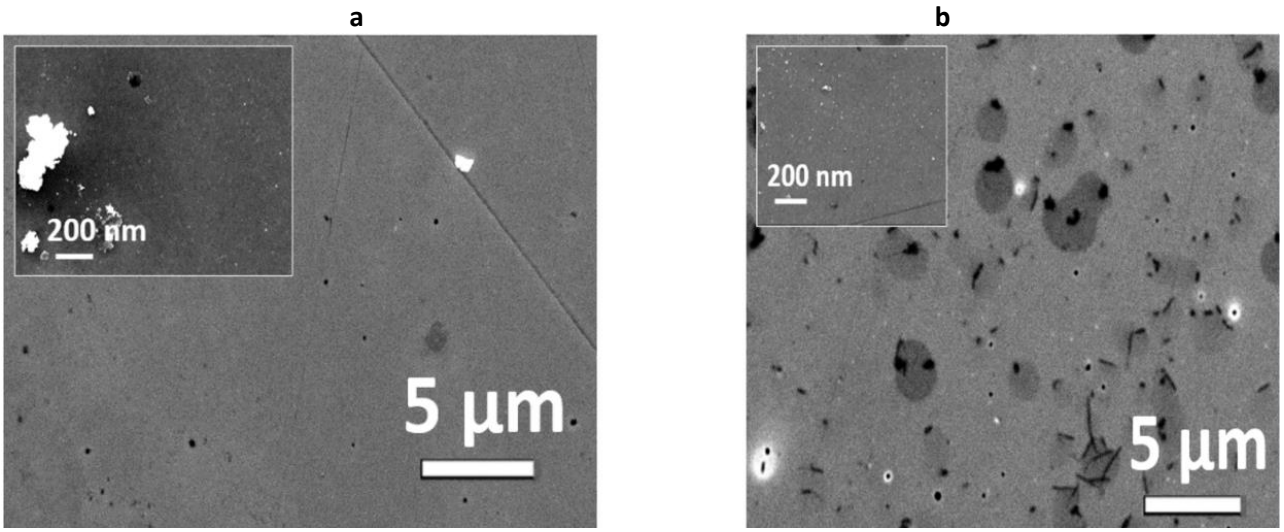

Figure 6. *Scanning electron microscopy (secondary electron) image of ASS 304L surface after different immersion times (a) t = 0 s, (b) t = 2 months*

The small particles (few nanometers size) with high bright contrast are likely relative to deposition of some dust coming from the air or the liquid. Some are also visible on the sample immersed for 2 months (Figure 6b).

However, an immersion for 2 months induced a clear change in the sample surface. The surface density of the dark contrast inclusions is higher on the observed zone: this may be attributed to the inhomogeneity of the initial material, as such an increase was not observed on the whole surface. However, it is not excluded that some new species (oxide precipitates, hole…) appeared during long immersion in liquid thanks to the pitting corrosion or oxidation. Around these small inclusions with full dark contrast (attributed to the sulfides inclusions in the initial surface), new areas with intermediate dark contrast were formed over few square micrometers after the immersion of 2 months.

Indeed, the sulfides inclusions (MnS) are demonstrated to play a major role in the corrosion behavior of stainless steels in (high concentration) NaCl solution, as favored locations to initiate the pitting corrosion [6,18]. Although the involved mechanism is still discussed, MnS inclusions would enable a preferential adsorption of chloride ions compared to the surrounding passivated *γ* phase. Depending on several factors (chloride ions concentration, shape and composition of inclusions…), this can lead to dissolution of the sulfides precipitates as well as the initiation of a preferential oxidation of the nearby material [19]. These changes naturally affect the electrochemical behavior of ASS 304L in OCP and EIS measurements.

Despite this visible change in surface morphology, the RMS roughness value measured on ASS 304L surface exposed to NaCl solution for two months was not changed. It remains about 25 ± 5 nm.

The XPS spectra and the deduced chemical analysis are presented in Figure 7 and Table 2.

The XPS results revealed that the same elements were detected for the film formed in the air, after immersion at t = 0 or t = 2 months. The main evolution with the immersion time is the variation of the Fe-total /Cr-total ratio: from the initial value of 0.58, the immersion first slightly increases it up to 0.69 but the 2 months' immersion induces reduction of the ratio to 0.23. The film is then significantly depleted in iron, probably by a phenomenon of iron hydroxides dissolution or a favored chromium oxide growth. Secondly, the Fe^0 contribution around 706 eV in the Fe $2p_{3/2}$ signal is modified by the immersion. Compared to the hydroxide/oxide peaks, its relative proportion (~28 %) is reduced to 15-19 % after immersion (Figure 7b and Table 2). This evolution, in conjunction with the aforementioned Fe/Cr ratio decrease, confirms the dissolution of Fe-hydroxide/oxide in the growing passive layer. Comparatively, no significant modification with immersion time can be observed in the shape of the Cr $2p_{3/2}$ peak (Figure 7c), with a clear predominance of Cr^{III}. The calculated thickness δ_{Ox} of the oxidized layer is not significantly evolving and remains roughly constant around 4 nm.

Finally, the altered thickness and chemistry of the passive oxide film, as well as the localized oxidation/corrosion pits observed by SEM, consequently involve the modifications of the physical/chemical surface properties. For instance, the electrical conductivity and also the interaction with species in the liquid (adsorption and desorption) are parameters that clearly influence the electric double layer (EDL) formation, its characteristics, and thus the electrical response in EIS measurements. The appearance of a second time constant in the phase Bode plot (Figure 5b) is then related to these modifications although additional simulation with an equivalent electrical circuit is required to link the observed modifications with the EIS results.

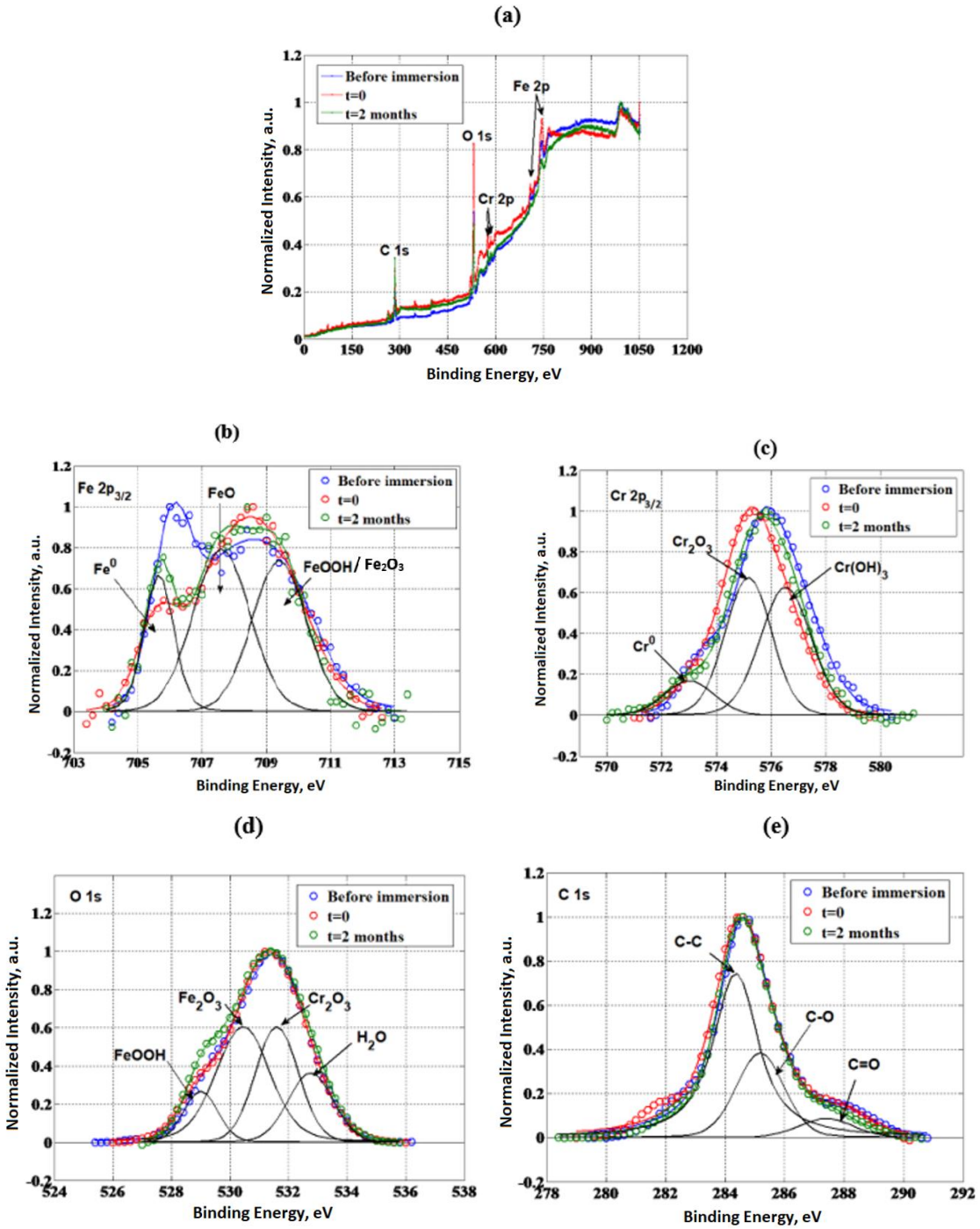

Figure 7 *(a) Low resolution and High resolution, (b) Fe 2p3/2, (c) Cr2p3/2, (d) O 1s, (e) C 1s XPS normalized spectra of the surface films formed on ASS 304L in the air and after different immersion times. Round dots are experimental data and the colored continuous lines are the simulated spectra. The black lines correspond to the different simulated contributions of the XPS spectra measured after a 2 months immersion (t=2 months)*

Conclusions

In the present work, the immersion time influence on the characteristics of the ASS 304L alloy in the NaCl solution (0.01M) was studied using surface analysis (OM, SEM, AFM, WLI, XPS) and electrochemical characterization techniques (EIS, OCP). The following conclusions can be drawn:

- With all the precautions taken concerning the metal samples preparation by polishing and well controlled manipulations, the repeatability deviation is 1 % but that of reproducibility is 35% for the EIS method. This poor reproducibility has been attributed to unstable surface states related

to transient phenomena or solid surface inhomogeneities. The OCP evolution with the immersion time is confirming the transient regime over at least several days.

- Surface characterization and electrochemical results proved that the long-term immersion modifies the composition and the electrochemical response of the ASS 304L surface. After two months solution immersion, the impedance diagrams show the appearance of a second time constant at low frequencies. It is attributed to the modifications of the oxide film properties and/or of the charge transfer in the EDL. Indeed, SEM and XPS analysis confirm a significant modification of the surface morphology (corrosion pits, localized oxidation) and an iron depletion (by dissolution) in the thicker passive oxide layer after long immersion times.

Acknowledgments: *This work was funded by the French Government program "Investissements d'Avenir" (LABEX INTERACTIFS, reference ANR-11-LABX-0017-01).*

References

[1] M. Ibrahim, S. S. Abd El Rehim, M. M. Hamza, *Materials Chemistry and Physics* **115** (2009) 80-85.
[2] L. J. Oblonsky, M. P. Ryan, H. S. Isaacs, *Journal of the Electrochemical Society* **145** (1998) 1922-1932.
[3] C. Olsson, D. Landolt, *Electrochimica Acta* **48** (2003) 1093-1104.
[4] L. Hamadou, A. Kadri, N. Benbrahim, *Applied Surface Science* **252** (2005) 1510-1519.
[5] M. Mohammadi, L. Choudhary, I. M. Gadala, A. Alfantazi, *Journal of the Electrochemical Society* **163** (2016) C883-C894.
[6] L. Freire, M. J. Carmezim, M. G. S. Ferreira, M. F. Montemor, *Electrochimica Acta* **56** (2011) 5280-5289.
[7] S. Fajardo, D. M. Bastidas, M. Criado, J. M. Bastidas, *Electrochimica Acta* **129** (2014) 160-170.
[8] A. Calmet, N. Vejar, X. Gonzalez, M. Sancy, A. Ringuede, V. Lair, S. Griveau, J. H. Zagal, F. Bedioui, M. Cassir, *Electroanalysis* **30** (2016) 162-169..
[9] B. R. Strohmeier, *Surface and Interface Analysis* **15** (1990) 51-56
[10] J. Lu, W. Sun, A. Becker, *Journal of Mechanical Sciences* **105** (2016) 315-329.
[11] L. Veleva, M. A. Alpuche-Aviles, M. K. Graves-Brook, D. O. Wipf, *Journal of Electroanalytical Chemistry* **537** (2002) 85-93.
[12] S. Tang, O. J. Kwon, N. Lu, H. S. Choi, *Surface and Coatings Technology* **195** (2005) 298-306.
[13] K. Brunelli, S. Gottardello, E. Napolitani, B. Dal Bianco, R. Bertocello, M. Magrini, M. Dabalà, *Materials Chemistry and Physics* **136** (2012) 1073-1080.
[14] J. Pellier, J. Geringer, B. Forest, *Wear* **271** (2011) 1563-1571.
[15] L. Freire, M. J. Carmezim, M. al Ferreira, M. F. Montemor, *Electrochimica Acta* **55** (2010) 6174-6181.
[16] C. Compere, N. Le Bozec, *Proceeding of the First Stainless Steel Congress in Thailand,* Thailand, **159** (1997) in EFC Working Party Report on 'Microbially Induced Corrosion'.
[17] I. Costa, C. V. Franco, C. T. Kunioshi, J. L. Rossi, *Corrosion* **62** (2006) 357-365.
[18] M. A. Baker, J. E. Castle, *Corrosion Science* **34** (1993) 667-682.
[19] P. Schmuki, H. Hildebrand, A. Friedrich, S. Virtanen, *Corrosion Science* **47** (2005) 1239-1250.